RSC Advances

ROYAL SOCIETY OF CHEMISTRY

www.rsc.org/advances

Effect of reducing coke of catalyst by La loading in hydrocracking of Jatropha oil

Fan Kai[1], Xiaoyi Yang[2], Jing Liu[3], Long Rong[1*]

1 Key Laboratory for Biomechanics and Mechanobiology of Ministry of Education, School of Biological Science and Medical Engineering, Beihang University, Beijing 100191, P R China

2 Energy and Environment international center, Beihang University, Beijing 100191, P R China

3 Beijing Key Laboratory of Lignocellulosic Chemistry, Beijing Forestry University, Beijing 100083, P. R. China

Abstract

In order to assess the La's effect of reducing carbonaceous deposition (coke) on catalyst for the hydrocracking of Jatropha oil, the NiW/nHA, NiW/Al_2O_3 and NiW/HY catalysts modified by La loading were synthesized and studied. The catalysts were characterized by N_2 adsorption-desorption, powder X-ray diffraction (XRD), X-ray photoelectron spectroscopy (XPS), temperature-programmed desorption of ammonia (NH_3-TPD), temperature programmed desorption of hydrogen (TPD-H_{ads}), temperature-programmed desorption of carbon dioxide (CO_2-TPD). The species and the amount of coke on the hydrocracking catalyst were measured by Fourier transform infrared (FT-IR), solid state ^{13}C nuclear magnetic resonance (NMR) and thermogravimetric analysis (TGA), demonstrating that the coke was constituted by polyaromatic hydrocarbon and that the La catalyst loading had a very positive effect on the coke reduction. The amount of coke on NiW/nHA, NiW/Al_2O_3 and NiW/HY catalyst decreased respectively by 0.94 %, 1.19%, 1.91 after 8h and 1.66%, 1.89%, 3.78% after 180h. The catalytic stability and the catalyst lifetime were also improved by La loading.

Keywords: La; Reducing coke; polyaromatic; Hydrocracking; Jatropha oil;

Introduction

In the past decades, the increasing world energy crisis and the growing concerns on environment protection have made the renewable biofuels an important alternative to the fossil fuel. [1, 2] There are many benefits of biofuel, such as high quality, decreased greenhouse gas emissions, decreased dependence on fossil fuel and increased national energy security. Hydrocracking of vegetable oil, which transformed triglyceride into hydrocarbons with hydrogen at elevated temperature and pressure in the presence of heterogeneous catalysts, is one of the processes widely used and studied for the production of new biofuels. [3, 4]

The common industrial catalysts for hydrocracking production are the alumina support and bifunctional catalyst (HY, HZSM, SAPO) with sulfurated transition metal (Ni, Mo, W) loading. [5-7] During the hydrocracking process, the produced carbonaceous deposition (coke) shall deposit on the catalyst. Although many research focused on improving the process of hydrocracking, few work was concerned with the formation of coke. As the amount of coke increased, it will cover the active center and block the catalyst pore, deactivating the catalyst in the long term reaction. For practical application, it is necessary to make detailed research about the mechanism of reducing coke formation.

In our previous work, the rare earth element La was used for getting rid of sulfur. [8] Finally, the effects of La loading not only lead to desulfuration, but also reduce the coke of catalyst. For seeking out this effect of reducing coke, traditional catalyst including the Al_2O_3 and HY should be

* Corresponding author. Tel: +86 10 8233 9157; fax: +86 10 8233 9157.
E-mail address: ronglong@buaa.edu.cn

tested in La loading. Besides, we also have successfully synthesized the nano-hydroxyapatite (nHA) for hydrocracking, [9] this support shall be tested whether it has the same effect. Thus, in this work, the La was loaded into NiW/Al_2O_3, NiW/nHA and NiW/HY catalyst for hydrocracking of Jatropha oil, the coke species shall be investigated and effect of reducing coke by La loading shall also be discussed.

Experimental

Catalyst preparation and characterization

The Al_2O_3 and nHA support were prepared by a precipitation method. [9, 10] All the chemical reagents used in this work were analytic reagent and purchased from Sinopharm Chemical Reagent Co., Ltd, China.

Al_2O_3: The $AlCl_3$ $6H_2O$ was dissolved in deionized water with ultrasonic, the ammonium hydroxide was used to adjust the pH to 10 under room temperature. After that, the stirring was continued for 1 hour with ultrasonic and keep the slurry aged for 12 hours, then washed with deionized water to pH 7. The obtained precipitate after centrifugation was calcined at 400 ℃ for 6h.

nHA: $Ca(NO_3)_2$ $4H_2O$ was dissolved in deionized water while Na_3PO_4 $6H_2O$ were dissolved in another deionized water. Then the Na_3PO_4 solution was titrated into the blend solution at a Ca/P molar ratio of 1.67 with mechanical stirred and ultrasonic processing at pH 10 under room temperature. After titration, the stirring was continued for 1 hour with ultrasonic and keep the slurry aged for 12 hours, then washed with deionized water to pH 7. The obtained precipitate after centrifugation was calcined at 400 ℃ for 6h.

The HY support was purchased from Catalyst Plant of Nankai University. The Ni, W, La (Ni 5.6%, W 6.4%, La 5%) component were loaded by impregnation of aqueous solutions of $Ni(NO_3)_2$ $6H_2O$, $(NH_4)_6W_7O_{24}$ $6H_2O$ and $La(NO_3)_3$ $6H_2O$. Impregnated samples were dried at 100 ℃ over night and calcined at 400 ℃ for 6h.

To determine specific surface areas, the N_2 adsorption-desorption were measured using a V-Sorb 2800 TP Surface Area and Pore Distribution Analyzer instrument (BeiJing Gold APP Instruments Co.,Ltd). At first, the samples were degassed in a vacuum at 300 ℃ for 4 h, then the specific surface area was obtained by the Brunauer, Emmett and Teller (BET) procedure. The t-plot method and Barret-Joyner-Halenda (BJH) method were used to determine the area of the micropores and pore size distribution, respectively.

The X-ray diffraction (XRD) patterns used Cu-Kα radiation at 40 kV and 30 mA, recording on a D/max2500VB2+/PC XRD analyzer (Japan Electronics Science Co.,Ltd.). The samples were measured at a scan speed of 2 °/min, in the 2θ range from 10 ° to 80 °.

X-ray photoelectron spectroscopy (XPS) measurements were carried out at 280 eV pass energy, using a ESCALAB 250Xi instrument (Thermofisher). Binding energies were corrected for sample charging, using the C 1s peak at 284.6 eV for adventitious carbon as a reference. The peak areas of the samples were determined by measuring the Ni 2p and W 4f peak areas (after linear subtraction of the background).

The temperature-programmed desorption of ammonia (NH_3-TPD) were using a TP-5080 Multi-functional automatic Adsorption Instrument (Tianjin Golden Eagle Technology Co.,Ltd) to determine the acidities of the catalysts. Before started, all samples were pretreated in N_2 (25 mL/min) at 300 ℃ for 2 h. The desorption step was performed at a heating rate of 10 ℃/min from 100 ℃ to 700 ℃.

Temperature programmed desorption of hydrogen (TPD-H_{ads}) experiments were performed using a TX 200 equipment from Tianjin Golden Eagle Technology Co.,Ltd., a mixed stream of H_2 (20 ml/min) and N_2 (38 ml/min) was used for 100 mg of catalyst samples. Adsorption of hydrogen was carried out initially at constant temperature of 200 ℃ for 0.25 h, then gradually decreasing temperature from the initial value to 20 ℃, finally at constant temperature of 20 ℃ for 1 h. After that, the examined sample was flushed with a N_2 stream (38 ml/min, 20 ℃, 0.25 h) to remove adsorbed hydrogen by TPD method. The TPD-H_{ads} examination was carried out in an N_2 stream of 38 ml/min at linearly increasing temperature of 10 ℃ /min from 20 to 900 ℃.

The CO_2-TPD measurement was used for surface basicity testing of catalyst samples. All samples (100 mg) were first treated in He at 400 ℃ for 1 h, cooled to 50 ℃. And then exposed to CO_2 (10 ml/min) for 0.5 h, purged in He for 2 h at 50 ℃ and heated linearly at 10 ℃ /min to 800 ℃ in 30 ml/min He. CO_2 (m/e = 44) in effluent was recorded continuously as functions of temperature.

The thermogravimetric analysis (TGA) were performed on a NETZSCH STA449F3 analyzer to determine the amount of coke on the past-reacted catalysts. Samples were first heated from 30 ℃ to 550 ℃ with a heating rate of 30 ℃ min^{-1} in N_2 flow of 100 ml min^{-1}, at a constant temperature of 550 ℃ for 15 min, then heated linearly at 30 ℃ min^{-1} to 800 ℃ in 100 ml min^{-1} O_2 flow. The weight loss of samples was calculated by microcomputer.

Chemical analysis of the fresh and used catalyst support were carried out by a Fourier transform infrared (FT-IR) spectrophotometer (GANGDONG FTIR-650) in the range from 4000 cm^{-1} to 400 cm^{-1} at 1.5 cm^{-1} resolution averaging 32 scans.

The solid-state ^{13}C NMR experiments were performed on Bruker AVANCE III 600 spectrometer at a resonance frequency of 150.9 MHz to analysis the component of coke on the catalyst. The ^{13}C NMR spectra were recorded using a 4 mm MAS probe and a spinning rate of 14 kHz. A contact time of 3 ms, a recycle delay of 5 s, and 4000 accumulations were used for the ^{13}C measurement. The chemical shifts of ^{13}C was externally referenced to TMS.

Catalytic activity measurements

Jatropha oil was purchased from Jiangsu Donghu Bioenergy Co., Ltd, the content includes: myristic acid 0.1%, arachic acid 0.5%, linolenic acid 0.9%, palmitoleic acid 1.2%, stearic acid 7.3%, palmitic acid 14.8%, linoleic acid 36.2%, oleic acid 38.3%.

The experiments were performed in a fixed-bed reactor equipped with electrically heating system. (JF-2, Tianjing Golden Eagle Technology Co., Ltd, China). The equipment for continuous hydrotreatment included feed system, heating section, tubular reactor, condensation section, storage section, instrumentation and control section. The reaction temperature was controlled by microcomputer while the system pressure was maintained by a back-pressure regulator. Jatropha oil was delivered from a feed pot into the reactor by a high-pressure pump. The hydrogen input rate was controlled by a separate mass-flow meter.

The catalyst samples (10g) were loaded respectively into the tubular reactor and activated prior to the experiments with H_2 flow at 400 ℃ and 3 MPa for 3h. The reaction conditions for catalytic hydrocracking experiment were as follows: temperature 360 ℃, pressure 3MPa, LHSV 2 h^{-1}, and H_2 to feed ratio of 600 mL H_2 gas/mL liquid feed.

After 8h of stabilization of reaction conditions, the product oil was analyzed by a gas chromatograph equipped with a flame-ionization detector (FID). The capillary column (AT.SE-30, Lanzhou Institute of Chemical Physics, Chinese Academy of Sciences) dimensions were 0.32 mm

i.d. × 30 m with a film thickness of 0.5 μm. The normal paraffin standards (purchased from Sigma–Aldrich, LLC) were used to estimate the relative percentages and distributions of the products with respect to their carbon numbers. The conversion of Jatropha oil was calculated as:

$$C = 100\% - C_{(JO)} \quad (1)$$

where $C_{(JO)}$ is the remaining Jatropha oil (%) in the products determined by GC analysis. The *n*-paraffin and *iso*-paraffin were calculated on the basis of GC analyzer program on microcomputer.

Results and discussion

Characterization of catalyst

The BET data of different catalysts were presented in Table 1. The nHA exhibited larger total pore volume (0.51 cm^3/g) and average pore diameter (22.3 nm), the HY had larger specific surface areas (452 m^2/g). The La loading amount (5%) was based on our previous work. After impregnation, all samples' specific surface areas and total pore volume decreased while the average pore diameter increased, suggesting some pores of catalysts were blocked by the metal La.

Table 1 Textural properties of catalysts

Catalyst	Specific surface areas, m^2/g	Total pore volume, cm^3/g	Average pore diameter, nm
nHA	161	0.51	22.3
NiWLa/nHA	114	0.43	23.1
Al_2O_3	378	0.54	5.6
NiWLa/Al_2O_3	325	0.49	6.4
HY	452	0.42	0.8
NiWLa/HY	397	0.38	0.9

The XRD patterns of different catalysts were shown in Fig. 1. All samples exhibited their own standard XRD spectrum of hydroxyapatite (JCPDS No. 9-0432), γAl_2O_3 (JCPDS No. 10-0425) and zeolite Y (JCPDS No. 81-2467), respectively. [11-13] After impregnation, the main crystal structure of catalysts remained, suggesting the frameworks of catalysts were undamaged. It was obvious that after impregnation of Ni and W, the diffraction peaks of Ni oxide phase (2θ = 37.3°, 43.6° and 63.4°, JCPDS No. 4-835) and WO_3 (2θ = 55.9°, JCPDS No. 43-1035) appeared at the figure, [14, 15] demonstrating the metal was successfully loaded. However, after impregnation of La, the La_2O_3 phase was considered to disperse highly on the surface, which is not detected by XRD. Meanwhile the peaks of NiO and WO_3 became weaker after La loading, indicating highly dispersion of Ni and W, this was in agreement with the reported literature by Bouarab et al. [16] Moreover, as the literature reported, the coke was supposed to occur more easily on larger metal particles than on smaller ones. [17] Therefore, the high dispersion of Ni, W could contribute to the resistance of coke.

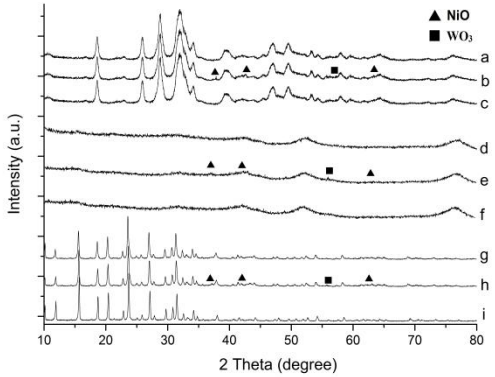

Fig. 1 XRD patterns of (a) nHA (b) NiW/nHA (c) NiWLa/nHA (d) Al_2O_3 (e) NiW/Al_2O_3 (f) NiWLa/Al_2O_3 (g) HY (h) NiW/HY and (i) NiWLa/HY

To investigate the variation of Ni and W oxidation state caused by La, the NiW and NiWLa were examined using XPS. The Ni 2p core level signal of NiW was shown in Fig. 2(a), the binding energy values at 851.2 and 852.6 eV were associated with the Ni^0 of NiW and NiWLa respectively, [18] other peaks were associated with the Ni^{2+}. The W 4f core level signal was shown in Fig. 2(b), the peaks of low binding energy value at 36.4 eV and 36.6 eV were attributed to W^{x+} (W^{x+} represents nonstoichiometric WO_x/W) of NiW and NiWLa respectively, other peaks at high energy values were attributed to W^{6+}.[19]

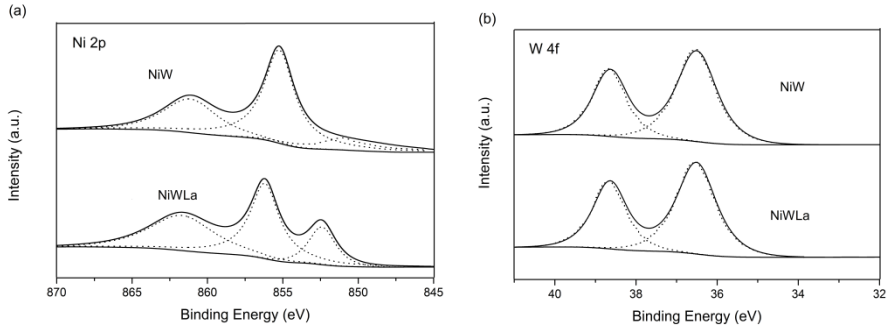

Fig. 2 XPS spectra of (a) Ni 2p and (b) W 4f

As calculated from Table 2, the content of the Ni^0 significantly increased after La loading. The ratio of Ni^0/Ni^{2+} was increased from 11.6% to 48.4%, while that of W^{x+}/W^{6+} was decreased from 55.5% to 43.9%. These demonstrated the La loading could promote the reduction of Ni^{2+} and the oxidation of W^{x+}, these also implied the W species donate partial electrons to Ni oxide species. Therefore, the reduction state of Ni increased, the hydrogenation capacity of catalysts were enhanced. [20, 21]

Table 2 Relative peak areas and ratios of Ni and W in the XPS analysis.

Catalyst	Ni (%)			W (%)		
	Ni^0	Ni^{2+}	Ni^0/Ni^{2+}	W^{x+}	W^{6+}	W^{6+}/W^{x+}
NiW	10.4	89.6	11.6	69.5	30.5	43.9
NiWLa	32.6	67.4	48.4	64.3	35.7	55.5

The NH_3-TPD profiles of different catalyst samples were shown in Fig. 3, the total acidities of them were recorded in Table 3. It can be concluded that before La loading, the acidities of catalysts followed the order: NiW/nHA<NiW/Al_2O_3<NiW/HY. The nHA and Al_2O_3 exhibited mild acidity while HY had strong acidity. After La loading, all the acidities of catalysts decreased.

It was probably due to some of the La cations replaced the framework cation (Al^{3+} and Ca^{2+}) to balance the negative framework charge by ion exchange, leading the original acidity of catalyst partly disappeared, this results were in accord with the reported literature. [22, 23]

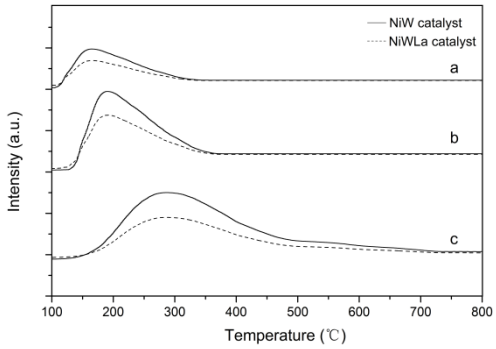

Fig. 3. NH_3-TPD profiles of (a) NiW/nHA and NiWLa/nHA (b) NiW/Al_2O_3 and NiWLa/Al_2O_3 (c) NiW/HY and NiWLa/HY

Table 2 Acidities of catalysts

Catalyst	Total acidity (mmol/g)
NiW/nHA	0.12
NiWLa/nHA	0.09
NiW/Al_2O_3	0.28
NiWLa/Al_2O_3	0.2
NiW/HY	0.97
NiWLa/HY	0.78

The TPD-H_{ads} was used to determinate the metal function (hydrogenation capacity) of catalysts. The TPD-H_{ads} spectra of catalysts were shown in Fig. 4, before La loading, it was obvious that there are two peaks, indicating two adsorbing sites on the surface of the catalysts. The low temperature desorption peaks are assigned to hydrogen on metallic Ni, while the high temperature desorption peaks are due to the H_2 spillover species absorbed on the region between the active sites and support. [24] After La loading, the area of the lower temperature peak gradually increased while the area of the high temperature peak increased but shifted to higher temperatures. The total amount of H_2 desorption increased, revealing that the La loading increased the hydrogenation capacity of catalyst. These were consistent with the reported literature by Hou et al. [25]

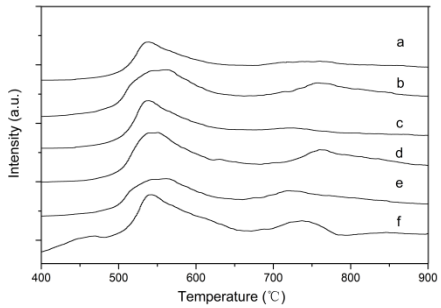

Fig. 4 TPD-H_{ads} spectra of (a) NiW/HY (b) NiWLa/ HY (c) NiW/Al_2O_3 (d) NiWLa/Al_2O_3 (e) NiW/nHA and (f) NiWLa/nHA

The CO_2-TPD profiles of different catalysts were shown in Fig. 5. Before La loading, little desorption peak of CO_2 can be only observed for NiW/nHA and NiW/Al_2O_3, it was due to the

alkalinity for both nHA and Al_2O_3 exhibiting. Yet the HY was typical acidy support, it had no absorption for CO_2. After La loading, it can be seen that the total amount of desorbed CO_2 obviously increased for all catalysts, indicating the corresponding basicity of catalysts was increasing due to La loading. Then the increased basicity of catalysts shall suppress the reaction, which need acid sites of catalyst to provide protons. [16, 26]

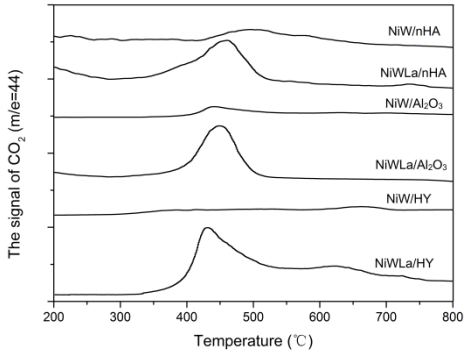

Fig. 5 CO_2-TPD profiles of different catalysts

Coke analysis

According to the reference of ISO 6964-1986, [27] the amount of coke on the used catalysts were determined by TGA. As shown in Fig. 6(A), the amount of coke on NiW catalyst after use for 8h was following the order: NiW/nHA<NiW/Al_2O_3<NiW/HY, the same with the acidity order of catalyst. After La loading, the coke amount on NiWLa catalyst after use for 8h was significantly lower than that on NiW catalyst, decreasing 1.91%, 0.94% and 1.19% than that on NiW/HY, NiW/nHA and NiWLa/Al_2O_3 respectively. As shown in Fig. 6(B), the data was similar with Fig. 6(A), the coke amount on all catalysts after use for 180h was also decreased 3.78%, 1.66% and 1.89 on NiW/HY, NiW/nHA and NiWLa/Al_2O_3, respectively.

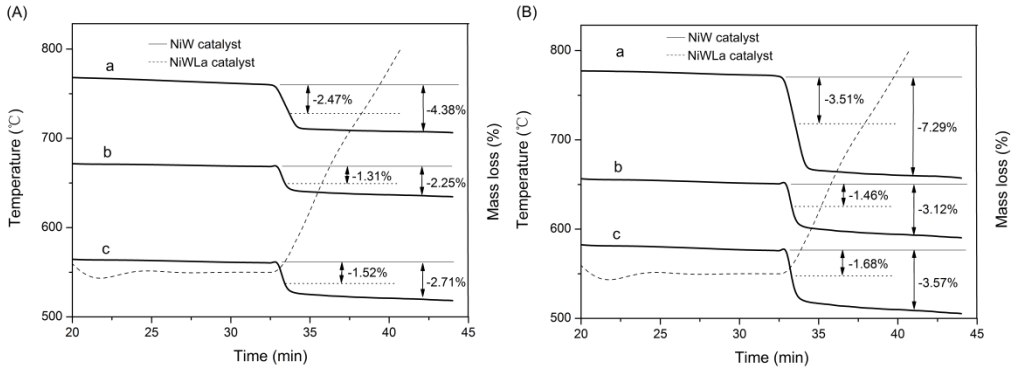

Fig. 6 TGA profiles of (a) NiW/HY and NiWLa/HY (b) NiW/nHA and NiWLa/nHA (c) NiW/Al_2O_3 and NiWLa/Al_2O_3 after use for (A) 8h and (B) 180h at 360 ℃, 3MPa, H_2/oil (v/v) = 600, LHSV=2 h^{-1}

The FT-IR spectrum of fresh and used catalysts were shown in Fig. 7. For the nHA, the characteristic peaks corresponding to OH^- (3434.2 and 627.3 cm^{-1}) and vibrations due to PO_4^{2-} (1105.3, 1031.9, 954.8, 601.8, 561.3, and 464.9 cm^{-1}) were observed. [28] For the Al_2O_3, the band at 3745.2 cm^{-1} is assigned to the OH vibration. For the HY, the intensity at 1700~2000 cm^{-1} was assigned to overtones and combination modes of the zeolitic framework. [29] It was obvious that the used catalysts all exhibited new bands at 1400~1600 cm^{-1} were characteristic of the vibration

absorption of C in aromatic rings, demonstrating the coke of hydrocracking catalyst was the polyaromatic compound. [30] Moreover, the signal of polyaromatic compound for used La loading catalyst was weaker, illustrating the coke amount was decreased, in accord with the TGA profiles.

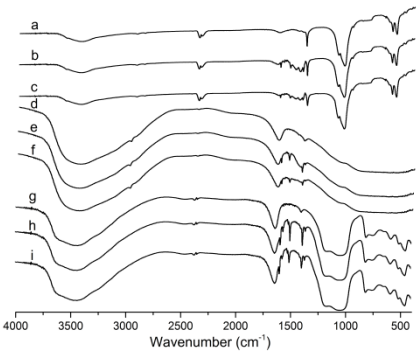

Fig. 7 The FT-IR spectrum of (a) NiW/nHA (b) used NiW/nHA (c) used NiWLa/nHA (d) NiW/Al_2O_3 (e) used NiW/Al_2O_3 (f) used NiWLa/Al_2O_3 (g) NiW/HY (h) used NiW/HY and (i) used NiWLa/HY

The ^{13}C NMR profiles of fresh and used catalysts were shown in Fig. 8. The used catalysts all exhibited new peaks around 125 ppm, corresponding to aromatic C–H bonds, while other peaks around 17 and 58 ppm were associated with the alkyl groups on the benzene ring. [31, 32] After La loading, the decreased signal of polyaromatic compound agreed with coke amount determinated by TGA. From these results, it can be proved again that the coke of hydrocracking catalyst is polyaromatic hydrocarbon and the La loading could reduce the coke amount.

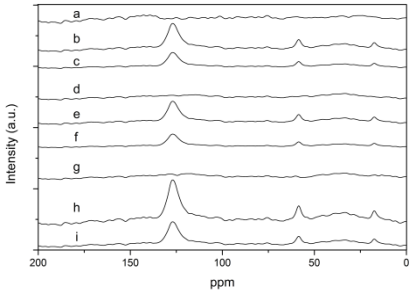

Fig. 8 The solid-state ^{13}C NMR profiles of (a) NiW/Al_2O_3 (b) used NiW/Al_2O_3 (c) used NiWLa/Al_2O_3 (d) NiW/nHA (e) used NiW/nHA (f) used NiWLa/nHA (g) NiW/HY (h) used NiW/HY and (i) used NiWLa/HY

Hydrocracking results

The GC charts of the product oil from hydrocracking of Jatropha oil over catalysts at 360 ℃, 3 MPa, H_2/oil (v/v) =600, LHSV=2 h^{-1} were shown in Fig. 9. Chemically, 3 mole fatty acid shall be produced from 1 mole of raw materials. As the literature had proved that after the oxygen removing reaction in hydrogen atmosphere, the fatty acid transformed to *n*-paraffins. [33] There are two routes of the oxygen removing, One is hydrodeoxygenation (HDO) yielding paraffins with even carbon number (mainly C16 and C18) and H_2O; the other is hydrodecarboxylation (HDC), including decarbonylation and decarboxylation, yielding paraffins with odd carbon number (mainly C15 and C17) and CO, CO_2.

After that, the isomerization of paraffins shall happen by the cooperation of metal and acid sites of catalyst. [34] According to the classical carbenium ion principle, the full process was as follows: I.

Through hydride elimination, the *n*-paraffin transformed to *n*-olefin. II. Carbenium ion intermediate was formed by proton addition. III. The formed normal carbenium ion intermediate isomerized to abranched carbenium ion intermediate. IV. The *iso*-olefin was formed by elimination of proton. V. Through hydrogenation, the *iso*-olefin transformed to *iso*-paraffin. However, at step III, the cracking reaction might happen, producing light paraffins. Therefore, as the GC charts illustrated, the main contents of product oil were *n*-paraffins and *iso*-paraffins ranging from C15~C18, besides, there are still some cracking light paraffins existing.

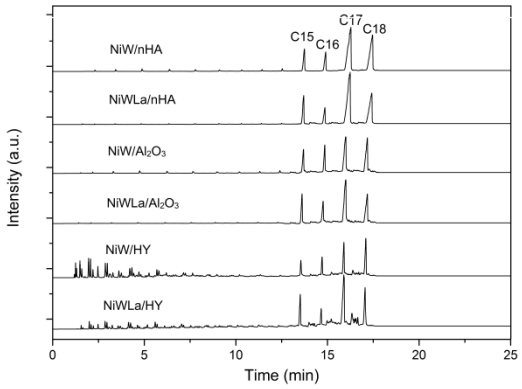

Fig. 9 GC charts of product oil over different catalysts at 360 ℃, 3MPa, H_2/oil (v/v) =600, LHSV=2 h^{-1}

As the literature reported, the formation of carbenium ion intermediates need proton, the isomerization reaction relates to the acidity of catalyst, [35, 36] it can be seen from Table 3, the cracking paraffins content decreased as the acidity of catalysts decreased after La loading. However, the *iso*/*n* ratio increased even if the acidity of catalyst dropped off, this fascinating phenomenon was also reported by Li et al, [37] the mechanism was due to the enhanced hydrogenation capacity and decreased acidity of catalyst caused by La loading, increasing the metal/acid function ratio. Then it suppressed the probability of the intermediates staying on an acid site and then the further cracking of the carbenium ion intermediates. Therefore, we inferred that the La loading could balance the metal/acid function ratio to enhance the isomerization and weaken cracking reaction.

Table 3 Hydrocracking of Jatropha oil over different catalysts at 360 ℃, 3MPa, H_2/oil (v/v) =600, LHSV=2 h^{-1}

Catalyst	NiW/nHA	NiWLa/nHA	NiW/Al_2O_3	NiWLa/Al_2O_3	NiW/HY	NiWLa/HY
Conversion (%)	89.3	100	78.4	95.2	82.3	92.4
Iso/*n* ratio	0.21	0.25	0.35	0.4	0.57	0.82
C15~C18	88.3	92.1	86.5	89.7	65.4	76.3
<C15	11.7	7.9	13.5	10.3	34.6	23.7

It was proved by FT-IR and solid-state ^{13}C NMR, the components of coke on the catalyst at high temperature were polyaromatic hydrocarbons. Based on the literature, [31, 32, 38, 39] the polyaromatic coke was formed from cracking paraffin, which was produced by cracking reaction of isomerization process. The cracking paraffin aromatization process can be divided in two parts. First, the cracking paraffin shall transform to olefin. Second, through oligomerization, cyclization and hydrogen transfer, the olefin shall transform to polyaromatic hydrocarbon, involving carbenium ions as transition states.

Since the acid/metal function was adjusted by La loading, the increased metal function could enhance the isomerization and weaken the cracking reaction, less cracking paraffin was obtained. On the other hand, as the NH_3-TPD and CO_2-TPD revealed, the acidity of catalyst was decreased while the alkalinity of catalyst was increased after La loading, it will slow down the formation of carbenium ion intermediate during aromatization process, suppressing the formation of polyaromatic hydrocarbon.

Reaction of time-on-stream

The conversion of Jatropha oil over different catalyst samples as a function of reaction time at 360 ℃, 3MPa, H_2/oil (v/v)=600, LHSV=2 h^{-1} were shown in Fig. 10. It was obvious that after La loading, all catalysts' conversion increased and remained constant, suggesting the catalytic stability can be improved by the La loading, this is consistent with Gao et al. [40] Combing with the TGA profiles, the coke of all catalyst samples decreased by La loading, avoiding the coke covering the active sites to deactivate the catalyst and guaranteeing the catalyst had a long lifetime for hydrocracking of Jatropha oil. Especially for the NiW/HY, its original strong acidity shall lead to more coke (over 5%), this is the reason of its conversion kept dropping off after use for 40h. After La loading, its coke amount evidently decreased, then the conversion became stable.

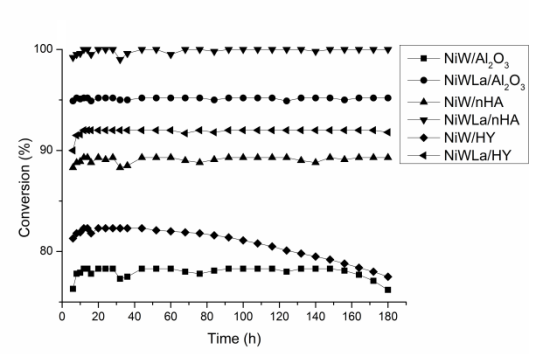

Fig. 10 Conversion of Jatropha oil over different catalysts at 360 ℃, 3MPa, H_2/oil (v/v) = 600, LHSV=2 h^{-1} as a function of reaction time

Conclusion

The La was respectively loaded into NiW/nHA, NiW/Al_2O_3 and NiW/HY catalyst to value its effect of reducing coke (polyaromatic hydrocarbon) in hydrocracking of Jatropha oil. In all cases, the amount of coke was significantly decreased by La loading. The La loading could enhance the hydrogenation capacity to reduce the obtained cracking paraffin, decrease the acidity and increase the alkalinity of catalyst to suppress the aromatization process. For long term reaction, the La loading kept conversion of Jatropha oil stable and extend the lifetime of catalyst.

References

1. G. W. Huber, P. O'Connor and A. Corma, *Applied Catalysis A: General*, 2007, 329, 120-129.
2. D. Kubička and L. Kaluža, *Applied Catalysis A: General*, 2010, 372, 199-208.
3. M. Krár, S. Kovács, D. Kalló and J. Hancsók, *Bioresource technology*, 2010, 101, 9287-9293.
4. R. Tiwari, B. S. Rana, R. Kumar, D. Verma, R. Kumar, R. K. Joshi, M. O. Garg and A. K. Sinha, *Catalysis Communications*, 2011, 12, 559-562.
5. R. Kumar, B. S. Rana, R. Tiwari, D. Verma, R. Kumar, R. K. Joshi, M. O. Garg and A. K. Sinha, *Green Chemistry*, 2010, 12, 2232-2239.
6. M. Toba, Y. Abe, H. Kuramochi, M. Osako, T. Mochizuki and Y. Yoshimura, *Catalysis today*,

2011, 164, 533-537.
7. A. Barrón C, J. Melo-Banda, J. Dominguez E, E. Hernández M, R. Silva R, A. Reyes T and M. Meraz M, *Catalysis Today*, 2011, 166, 102-110.
8. J. Liu, C. Liu, G. Zhou, S. Shen and L. Rong, *Green Chemistry*, 2012, 14, 2499-2505.
9. G. Zhou, Y. Hou, L. Liu, H. Liu, C. Liu, J. Liu, H. Qiao, W. Liu, Y. Fan and S. Shen, *Nanoscale*, 2012, 4, 7698-7703.
10. P. Priecel, L. Čapek, D. Kubička, F. Homola, P. Ryšánek and M. Pouzar, *Catalysis Today*, 2011, 176, 409-412.
11. J. Hu, J. Russell, B. Ben-Nissan and R. Vago, *Journal of materials science letters*, 2001, 20, 85-87.
12. D. Martin and D. Duprez, *The Journal of Physical Chemistry*, 1996, 100, 9429-9438.
13. D. Jin, B. Zhu, Z. Hou, J. Fei, H. Lou and X. Zheng, *Fuel*, 2007, 86, 2707-2713.
14. T. Hayakawa, S. Suzuki, J. Nakamura, T. Uchijima, S. Hamakawa, K. Suzuki, T. Shishido and K. Takehira, *Applied Catalysis A: General*, 1999, 183, 273-285.
15. S. Pokhrel, C. E. Simion, V. S. Teodorescu, N. Barsan and U. Weimar, *Advanced Functional Materials*, 2009, 19, 1767-1774.
16. R. Bouarab, O. Cherifi and A. Auroux, *Thermochimica acta*, 2005, 434, 69-73.
17. E. Ruckenstein and H. Wang, *Journal of Catalysis*, 2002, 205, 289-293.
18. T. Lehmann, T. Wolff, V. Zahn, P. Veit, C. Hamel and A. Seidel-Morgenstern, *Catalysis Communications*, 2011, 12, 368-374.
19. A. Vimont, A. Travert, C. Binet, C. Pichon, P. Mialane, F. Sécheresse and J.-C. Lavalley, *Journal of Catalysis*, 2006, 241, 221-224.
20. M. J. Ledoux and B. Djellouli, *Applied Catalysis*, 1990, 67, 81-91.
21. Y. Yoshimura, H. Shimada, T. Sato, M. Kubota and A. Nishijima, *Applied Catalysis*, 1987, 29, 125-140.
22. A. Yasukawa, K. Gotoh, H. Tanaka and K. Kandori, *Colloids and Surfaces A: Physicochemical and Engineering Aspects*, 2012, 393, 53-59.
23. M. Jiang, 1997.
24. J. B. Zheng, Z. Q. Xia, J. J. Li, W. K. Lai, X. D. Yi, B. H. Chen, W. P. Fang and H. L. Wan, *Catalysis Communications*, 2012, 21, 18-21.
25. Y. Hou, Y. Wang, F. He, S. Han, Z. Mi, W. Wu and E. Min, *Materials Letters*, 2004, 58, 1267-1271.
26. J. Gao, Z. Hou, J. Guo, Y. Zhu and X. Zheng, *Catalysis today*, 2008, 131, 278-284.
27. J. Zhu, X. Peng, L. Yao, J. Shen, D. Tong and C. Hu, *International Journal of Hydrogen Energy*, 2011, 36, 7094-7104.
28. R. Chakraborty and S. K. Das, *Industrial & Engineering Chemistry Research*, 2012, 51, 8404-8414.
29. B. Xu, F. Rotunno, S. Bordiga, R. Prins and J. A. van Bokhoven, *Journal Of Catalysis*, 2006, 241, 66-73.
30. C. L. Li, O. Novaro, E. Munoz, J. L. Boldu, X. Bokimi, J. A. Wang, T. Lopez and R. Gomez, *Applied Catalysis a-General*, 2000, 199, 211-220.
31. M. A. Callejas, M. T. Martinez, T. Blasco and E. Sastre, *Applied Catalysis a-General*, 2001, 218, 181-188.
32. H. S. Cerqueira, G. Caeiro, L. Costa and F. R. Ribeiro, *Journal Of Molecular Catalysis*

a-Chemical, 2008, 292, 1-13.

33. Y. Liu, R. Sotelo-Boyás, K. Murata, T. Minowa and K. Sakanishi, *Energy & Fuels*, 2011, 25, 4675-4685.
34. T. Degnan and C. Kennedy, *AIChE journal*, 1993, 39, 607-614.
35. M. Roussel, S. Norsic, J.-L. Lemberton, M. Guisnet, T. Cseri and E. Benazzi, *Applied Catalysis A: General*, 2005, 279, 53-58.
36. M. Roussel, J.-L. Lemberton, M. Guisnet, T. Cseri and E. Benazzi, *Journal of Catalysis*, 2003, 218, 427-437.
37. D. Li, F. Li, J. Ren and Y. Sun, *Applied Catalysis A: General*, 2003, 241, 15-24.
38. M. Guisnet and P. Magnoux, *Applied Catalysis a-General*, 2001, 212, 83-96.
39. G. Caeiro, R. H. Carvalho, X. Wang, M. Lemos, F. Lemos, M. Guisnet and F. R. Ribeiro, *Journal Of Molecular Catalysis a-Chemical*, 2006, 255, 131-158.
40. J. Gao, Z. Hou, J. Guo, Y. Zhu and X. Zheng, *Catalysis Today*, 2010, 151, 412-412.